

Mean kinetic energy of helium atoms in fluid ^3He and ^3He – ^4He mixtures

C Andreani, C Pantalei and R Senesi

Università degli Studi di Roma 'Tor Vergata', Dipartimento di Fisica and CNR-INFM, Via della Ricerca Scientifica 1, 00133 Roma, Italy

E-mail: carla.andreani@roma2.infn.it

Received 9 January 2006, in final form 12 April 2006

Published 2 June 2006

Online at stacks.iop.org/JPhysCM/18/5587

Abstract

Momentum distributions and mean kinetic energies of helium atoms, in pure fluid ^3He and ^3He – ^4He mixtures, at $T = 2$ K and ^3He concentrations of $x = 0.20$ and $x = 1.00$, are presented. The experimental technique employed is deep inelastic neutron scattering measurements in the eV energy range, with wavevector transfer of typically $100 \text{ \AA}^{-1} < q < 250 \text{ \AA}^{-1}$. Single-particle dynamical properties of ^3He – ^4He mixtures are discussed in the context of previous results on mixtures at different concentrations and pure ^3He and ^4He . In the pure fluids, the kinetic energy of ^3He and ^4He are remarkably similar for molar volumes above $25 \text{ cm}^3 \text{ mol}^{-1}$, while for smaller molar volumes, upon approaching the liquid–solid transition, the kinetic energy is larger in ^3He than ^4He . On the other hand, the short-time dynamics of the helium mixture reveal quite a different picture with respect to the pure ^3He and ^4He : the momentum distribution and mean kinetic energy of the light helium component are independent of the molar volume and concentration.

1. Introduction

The single-particle dynamics of ^3He and ^4He – ^3He mixture has been measured via inelastic neutron scattering measurements. Results of this work are discussed in the context of previous measurements on the same systems. Helium, due to its light mass, occupies a special role in condensed matter. Indeed, condensed ^4He , ^3He and helium isotopic mixtures represent the simplest prototype examples of many-body systems, i.e. interacting bosons and fermions with the same interparticle interactions, and interacting bosons–fermions with variable Fermi temperature. An outstanding example is the low-temperature superfluid behaviour of liquid ^4He , where the superfluidity is associated with Bose condensation of a macroscopic fraction of the helium atoms into a zero-momentum state. On the other hand, condensed ^3He is the prototype of a fermion many-body system, being the only neutral Fermi liquid (or solid)

accessible in nature. Although the inter-particle potential is known very accurately, ${}^3\text{He}$ still appears to be a challenge for theoreticians, because of the intrinsic difficulty in dealing with a many-body anti-symmetric wavefunction in quantum-mechanical simulations [1]. In the case of fluid helium mixture, the addition of ${}^3\text{He}$ atoms to ${}^4\text{He}$ mixes up the different statistics and modifies the molar volume of the system, thus introducing the ${}^3\text{He}$ concentration, x , as a new degree of freedom [1]. The latter provides new insight into the understanding of the interplay between interactions and quantum statistics. In recent years, several inelastic neutron scattering studies at high wavevector transfer have been performed on liquid and solid ${}^3\text{He}$ and ${}^4\text{He}$, and on ${}^3\text{He}$ - ${}^4\text{He}$ mixtures. In these systems, deep inelastic neutron scattering (DINS) measurements provide direct information about single-particle dynamical properties, such as the momentum distribution, $n(p)$, and the mean kinetic energy, $\langle E_K \rangle$. These quantities are generally compared with theoretical predictions from quantum Monte Carlo simulations and *ab initio* calculations. The aim is to effectively test theoretical predictions of the Bose condensate fraction in liquid ${}^4\text{He}$, density and temperature dependence of kinetic energies, and momentum distributions of liquid and solid ${}^4\text{He}$ and ${}^3\text{He}$ [2, 3]. The DINS technique, also known as Neutron Compton scattering [4], shares theoretical analogies with Compton scattering, i.e. the measurement of the electron momentum distribution by the scattering of high-energy photons. Within the framework of the *impulse approximation* (IA) [3], the DINS response function is the *neutron Compton profile* (NCP), $J(y, \hat{q})$, which represents the probability density distribution of y , the atomic momentum component along the direction of wavevector transfer \hat{q} . The quantity $y = \frac{M}{\hbar q}(\omega - \frac{\hbar q^2}{2M})$ is the West scaling variable [4, 2], M is the atomic mass of the struck nucleus, and $\hbar\omega$ is the energy transfer. The relation between the dynamical structure factor $S(\mathbf{q}, \omega)$ and the response function is expressed by:

$$\begin{aligned} S_{\text{IA}}(\mathbf{q}, \omega) &= \int n(\mathbf{p}) \delta\left(\omega - \frac{\hbar q^2}{2M} - \frac{\mathbf{q} \cdot \mathbf{p}}{M}\right) d\mathbf{p} \\ &= \frac{M}{\hbar Q} J(y, \hat{q}) \end{aligned} \quad (1)$$

which is exact in the limit of infinite wavevector transfer. In an isotropic liquid there is no dependence on the direction of the wavevector transfer \hat{q} and the response function becomes:

$$J(y) = 2\pi\hbar \int_{|hy|}^{\infty} pn(p) dp. \quad (2)$$

Values of $\langle E_K \rangle$ are obtained using the second moment sum rule for $J(y)$ [4, 5]:

$$\int_{-\infty}^{\infty} y^2 J(y) dy = \sigma_y^2 = \frac{2M}{3\hbar^2} \langle E_K \rangle \quad (3)$$

where σ_y is the standard deviation of the response function. Accurate DINS measurements, performed on fluid and solid ${}^4\text{He}$ [5, 6] and ${}^3\text{He}$, have provided successful benchmark tests of advanced theoretical models of many-body systems [3]. In the former system, for example, the experimental $n(p)$ are in quite good agreement with path integral Monte Carlo (PIMC) simulation. In the case of liquid and solid ${}^3\text{He}$, the experimental values of $\langle E_K \rangle$ are found to be in remarkable agreement with results from diffusion Monte Carlo simulation [3, 7, 8], which is the only theoretical calculation, among those currently available, which includes three-body interactions. On the other hand, in the case of liquid ${}^4\text{He}$ - ${}^3\text{He}$ mixture, several DINS investigations reveal a striking disagreement with theoretical values of the condensate fraction of the boson component, and of the $\langle E_K \rangle$ and $n(p)$ of the fermion component [3]. In particular, the kinetic energy, $\langle E_K \rangle_3$, of ${}^3\text{He}$ in the mixtures is found to be independent of both the ${}^3\text{He}$ concentration, x , and the molar volume, V_m . This finding does not support a general and accepted picture of the microscopic short-time dynamics in a quantum fluid, where the

mean kinetic energy is expected to be strongly dependent on the number density of the local environment around a single atom. A concentration-dependent local dilation around a ^3He atom is a possible mechanism invoked to explain that values of mean kinetic energies in the mixture are independent of concentration and molar volume [3]. Results of momentum distribution and mean kinetic energy studies on pure ^4He and ^3He from DINS experiments are briefly reviewed. New and recent experiments on the liquid mixtures will also be discussed, with a focus on the short-time dynamics of the ^3He atomic component in the mixture.

2. Measurements on pure ^4He and ^3He

Early DINS measurements on fluid ^4He [9] were devoted to the understanding of the changes occurring in the dynamical properties as the system goes from the quantum regime to the classical regime. Measurements at constant temperature were carried out along a supercritical isochore, at a density value of $n = (0.15 \pm 0.01) \text{ g cm}^{-3}$, close to the value at the lambda transition, up to a temperature of 50 K, where the system is expected to behave classically. Five measurements were performed in the temperature range 4.2–50 K, up to a maximum pressure of 23.3 MPa. Clear deviation from classical behaviour were shown at the lowest temperatures, while at high temperature the experimental results were well described within the classical model. The $\langle E_K \rangle$ for the zero-point motion, derived within the Einstein harmonic model, yielded a value of $(15.2 \pm 1.2) \text{ K}$, in good agreement with PIMC results [10] and reactor measurements [11]. A remarkable experimental and theoretical effort has also been devoted to the study of the molar volume dependence of $\langle E_K \rangle$ on helium in condensed phases. This is expected to be a direct consequence of the Heisenberg principle, i.e. fluctuations in momentum space increase by decreasing the volume where the atomic wavefunction is confined, thus producing an increase in mean kinetic energy. In condensed helium, both liquid and solid phases can be accessed, at the same molar volume, through appropriate conditions of pressure and temperature [12]. Moreover, the various degrees of local spatial order among liquid and solid phases are expected to result in a different density dependence of $\langle E_K \rangle$. In a detailed PIMC calculation performed on fluid and solid ^4He at 4 K [13] it was shown that, at constant density, a reduction in the mean kinetic energy is observed upon going from the liquid to the solid. In the DINS study by Bafle *et al* [14], the 4.35 K isotherm has been investigated for six and nine densities in the liquid and solid *hcp* phases, respectively. The density dependence in the liquid phase was well represented by a parabola, while the solid phase data were well described by a first-degree polynomial. A DINS measurement of the $n(p)$ lineshape in the normal phase (close to the lambda transition) and the superfluid phase [6] has shown a non-Gaussian component of the momentum distribution, in agreement with the PIMC calculation [13]. As far as condensed ^3He is concerned, due to the high helium absorption cross section, σ_a , inelastic neutron scattering experiments were limited to the liquid phase only. Indeed, the values of σ_a , for thermal neutrons, is of the order of 5000 barn, compared to a scattering cross section of about 6.9 barn. DINS measurements performed in the liquid phase have proven to be a very sensitive test of the $n(p)$ lineshape and single-particle properties derived from theoretical models [15, 16]. In principle, DINS measurements can also provide important information on the fermionic nature of $n(p)$, i.e. on the characteristic discontinuity at the Fermi momentum $p_F = \hbar(3\pi^2)^{1/3}n^{1/3}$. However, at present, this still represents an unsolved experimental challenge. An inelastic neutron scattering study of the fermionic nature in ^3He [17] indicated that the experimental $n(p)$ lineshape is compatible with both Gaussian and fermionic models. It is well known that, for temperatures above absolute zero, the sharp changes in the slope of $J(y)$ at $y = p_F/\hbar$ are progressively washed out. At the same time, $J(y)$ is expected to retain a non-Gaussian character, as in normal liquid ^4He [2]. Theoretical studies on liquid ^3He at

absolute zero temperature, by Mazzanti *et al* [18], provided the momentum distribution and the dynamical structure factor at wavevector transfer $q = 19.4 \text{ \AA}^{-1}$. These calculations included terms that accounted for the interactions of the struck atom with the medium, beyond the IA, known as final state effects (FSE) [3]. Novel DINS measurements on pure ^3He at $T = 2.00 \text{ K}$ and saturated vapour liquid pressure have been performed on the VESUVIO spectrometer at the ISIS pulsed neutron source, at values of $q \simeq 130 \text{ \AA}^{-1}$. This experiment has been carried out employing a subset of the backscattering detector array corresponding to a solid angle of approximately 0.31 sr. We stress that the current set-up, which will be completed by June 2006, will allow a detection solid angle of approximately 1.73 sr. Recent improvements in the spectrometer resolution have allowed a quantitative lineshape analysis on the neutron Compton profiles. For high q values, i.e. $q \simeq 100 \text{ \AA}^{-1}$, it is expected that the only relevant term of the final state effects is antisymmetric in y -space and is well accounted for by symmetrizing the response function around $y = 0$. However, previous results of DINS measurements on fluid ^4He and ^3He carried out with typical wavevector transfers $100 \text{ \AA}^{-1} < q < 140 \text{ \AA}^{-1}$ have shown that FSE are negligible and do not affect the peak shape significantly [19, 7]. As in the case of normal liquid ^4He [2, 6], the ^3He NCP can be described by a model lineshape consisting of a Gaussian with an additive kurtosis term of the following form:

$$J(y) = \frac{1}{\sqrt{2\pi}\sigma^2} \exp\left(-\frac{y^2}{2\sigma^2}\right) \left[1 + \frac{\delta}{8} \left(1 - \frac{2y^2}{\sigma^2} + \frac{y^4}{3\sigma^4}\right)\right] \quad (4)$$

where σ is the standard deviation of the NCP and δ is a kurtosis parameter. The present measurements have confirmed the presence of these non-Gaussian components in the momentum distribution. Using equation (4), one obtains the values of $\sigma = (0.70 \pm 0.04) \text{ \AA}^{-1}$ and $\delta = 0.99 \pm 0.40$, which are in good agreement with the theoretical predictions [18]. These values, in particular the kurtosis component, indicate a more pronounced non-Gaussian character in ^3He than in normal liquid ^4He [6] (where $\delta = 0.63$). Figure 1 reports the NCP obtained by employing two different energy analysers, namely ^{181}Ta foils of a thickness of (a) 25 μm and (b) 75 μm . The corresponding instrumental resolutions (c) show the increased performance of the instrument in terms of lineshape analysis and momentum distribution determination. The lineshape analysis of the experimental Compton profile was carried out by simultaneously fitting the resolution-broadened model function of equation (4) to the two spectra obtained by employing ^{181}Ta analyser foils of 25 and 75 μm thickness, respectively. Due to the detection solid-angle limitations, no attempt has been made to analyse data recorded with the double difference acquisition mode [20, 21] which, in the analyser foil configuration employed, requires a factor of 1.7 more counting statistics with respect to the single difference configuration [20]. Data analysis has been carried out with and without a symmetrization of the response functions, as shown above, in order to remove residual final-state effects contributions. The resulting NCP parameters, i.e. σ and δ , were the same for the two cases, within their respective uncertainties. We stress that this finding is in agreement with the fact that, for wavevector transfer of $q = 130 \text{ \AA}^{-1}$, final-state effect contributions are almost negligible. The residual discrepancies in the tail region between the best-fit lineshapes and the experimental response functions should, in our opinion, be attributed to data noise only. Figure 2 shows the experimentally reconstructed NCP, employing the model lineshape of equation (4) and the zero-temperature theoretical result from [18]. It has to be stressed that remarkable agreement between the theoretical and experimental determinations is found, the small differences being most probably due to temperature effects on the longitudinal momentum distribution. As far as solid ^3He is concerned, the first experimental determination of single-particle mean kinetic energies, $\langle E_K \rangle_3$, was carried out in 2001 [7]. In the same experiment, $\langle E_K \rangle_3$ was also derived in the high-density liquid. In the experiment, performed at a constant temperature of 2.00 K,

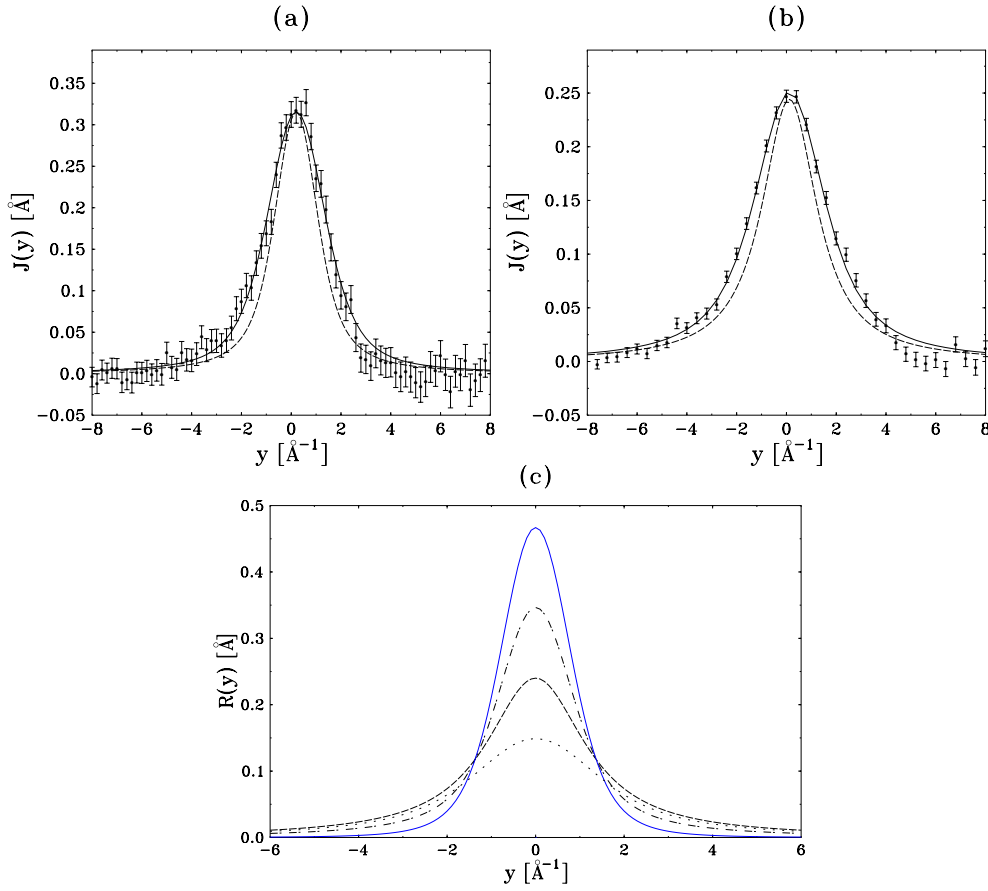


Figure 1. Neutron Compton profiles of pure liquid ^3He at $T = 2.00$ K and equilibrium pressure: (a) experimental data (circles with error bars) employing a ^{181}Ta analyser foil of $25\ \mu\text{m}$ thickness; best fit using the equation (4) (continuous line); resolution function (dashed line); (b) experimental data employing a ^{181}Ta energy analyser foil of $75\ \mu\text{m}$ thickness (circles with error bars); best fit using equation (4) convoluted with the spectrometer resolution function (continuous line); resolution function (dashed line). (c) Resolution functions on VESUVIO obtained by employing different energy analysers: ^{197}Au foil of $10\ \mu\text{m}$ thickness (dotted line); ^{181}Ta foil of $75\ \mu\text{m}$ thickness (short-dashed line); ^{181}Ta foil of $25\ \mu\text{m}$ thickness (dashed line); ^{181}Ta foils of $25\ \mu\text{m}$ and $75\ \mu\text{m}$ thicknesses, employing the double difference method [3] (continuous line).

(This figure is in colour only in the electronic version)

the applied pressure was varied in order to obtain a high-density liquid sample, a body centred cubic (*bcc*) and a hexagonal closed packed (*hcp*) sample of ^3He . The molar volume dependence of the $\langle E_K \rangle_3$ observed is in remarkable agreement with diffusion Monte Carlo calculations for both phases [8]. A summary of experimental determinations of the molar volume dependence of $\langle E_K \rangle$ for pure ^3He and ^4He samples is reported in figure 3. The experimental data for pure ^4He and ^3He are from [22, 23] and [24, 7], respectively. It is interesting to note that, in the molar volume range $25\ \text{cm}^3\ \text{mol}^{-1} \leq V_m \leq 40\ \text{cm}^3\ \text{mol}^{-1}$, the kinetic energies $\langle E_K \rangle_3$ and $\langle E_K \rangle_4$ for ^3He and ^4He are similar, while for $V_m \leq 23\ \text{cm}^3\ \text{mol}^{-1}$, $\langle E_K \rangle_3 > \langle E_K \rangle_4$. In particular, we stress that, considering a linear interpolation for the pure ^4He , we obtain the following values: $\langle E_K \rangle_4 = 29.7\ \text{K}$ for $V_m = 18.75\ \text{cm}^3\ \text{mol}^{-1}$, and $\langle E_K \rangle_4 = 26.05\ \text{K}$ for $V_m = 20.10\ \text{cm}^3\ \text{mol}^{-1}$,

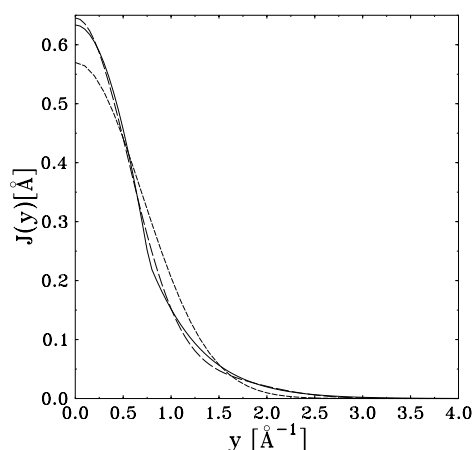


Figure 2. Neutron Compton profile of liquid ${}^3\text{He}$ at $T = 2.00$ K determined from: the present measurements, dashed line; Gaussian component, short-dashed line; and zero-temperature diffusion Monte Carlo results [18], solid line.

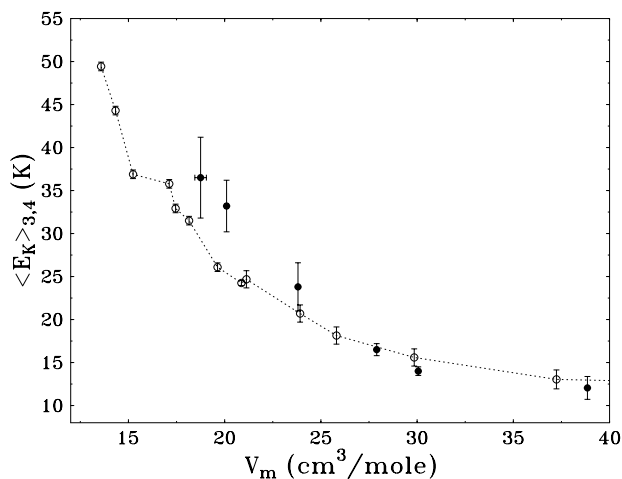


Figure 3. Molar volume dependence of mean kinetic energy for pure ${}^3\text{He}$ (full circles) from [24, 7], and pure ${}^4\text{He}$ (open circles) from [22, 23], respectively. The dashed line is a guide to the eye illustrating the molar volume dependence of the ${}^4\text{He}$ kinetic energy.

to be compared with the values $\langle E_K \rangle_3 = 36.5 \pm 4.7$ K and $\langle E_K \rangle_3 = 33.2 \pm 3.0$ K, respectively. These small molar volumes correspond to the high-density liquid and solid phases; here it is expected that quantum statistics play a minor role and differences in the kinetic energies are mainly due to the localization of atoms of different mass (${}^3\text{He}$ and ${}^4\text{He}$). In contrast, in the fluid phases, far from melting, exchange effects are relevant and appear to reduce $\langle E_K \rangle_3$ to values similar to $\langle E_K \rangle_4$. Accurate measurements of $\langle E_K \rangle_3$ in an extended molar volume range would be very important in order to obtain a comprehensive picture of the molar volume dependence of these quantum systems.

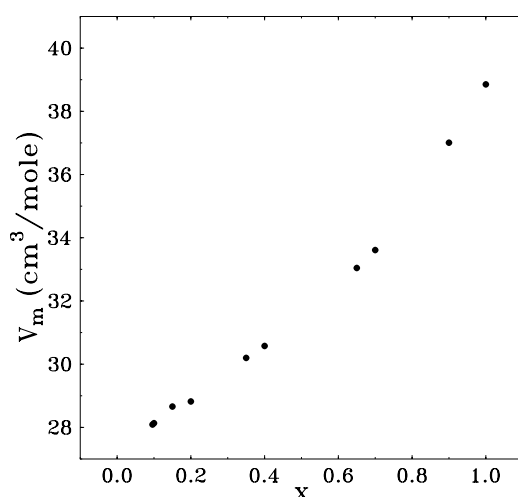


Figure 4. Concentration-dependent molar volume of ^3He - ^4He mixtures at equilibrium pressure at $T = 1.9$ K [25].

3. Measurements on ^3He - ^4He mixtures

Studies of ^3He - ^4He mixture are motivated by the interest in understanding the dynamical properties of a system characterized by the interplay between Fermi (^3He) and Bose (^4He) statistics, the interatomic interaction of the different helium atoms and the quantum-mechanical zero-point motion. The addition of ^3He to liquid ^4He results in a variety of physical macroscopic and microscopic properties, such as the concentration-dependent molar volume, finite miscibility at zero temperature, suppression of superfluidity, and enhancement of the condensate fraction [1]. Figure 4 shows the molar volume as a function of the ^3He concentration, x , for a mixture at equilibrium pressure for $T = 1.9$ K [25].

Experimental DINS results have revealed significant and interesting discrepancies between theory and experiments as far as the determination of the condensate fraction in the superfluid phase, the mean kinetic energy $\langle E_K \rangle_3(x)$ of the lighter isotope, and the momentum distributions are concerned [26, 27]. These findings provide useful information on the microscopic dynamics of the helium systems in addition to the remarkable agreement found between theory and experiments for pure high-density liquid and solid ^3He [7, 28, 8, 1] and pure fluid and solid ^4He [5, 12, 14, 29].

The single-particle mean kinetic energies $\langle E_K \rangle_{3,4}(x)$ reflect the localization of the two isotopes in the mixtures and are influenced by the mixture concentration. Experimental results from a recent DINS measurement, performed on the VESUVIO spectrometer at $T = 2.00$ K and ^3He concentrations $x = 0.20$ and 1.00 , are reported in table 1 (in bold) and figure 5. In table 1, results from previous inelastic measurements on the ^3He - ^4He mixtures, in a wide range of concentrations [26, 27, 30], are also listed. Figure 5 shows the experimental mean kinetic energies of He atoms as a function of molar volumes for these measurements. The results of the present study confirm that, at the concentration values of the experiment, the $\langle E_K \rangle_3(x)$ value is independent of x . This finding supports the important conclusion of the whole set of previous measurements in the concentration range $0.0 \leq x \leq 0.9$ [26, 27], that is, the local environment of the ^3He atoms in the mixtures is similar to that found in pure liquid ^3He at equilibrium conditions. Figure 6 illustrates the different behaviour of $\langle E_K \rangle_3$ as a function of V_m in the

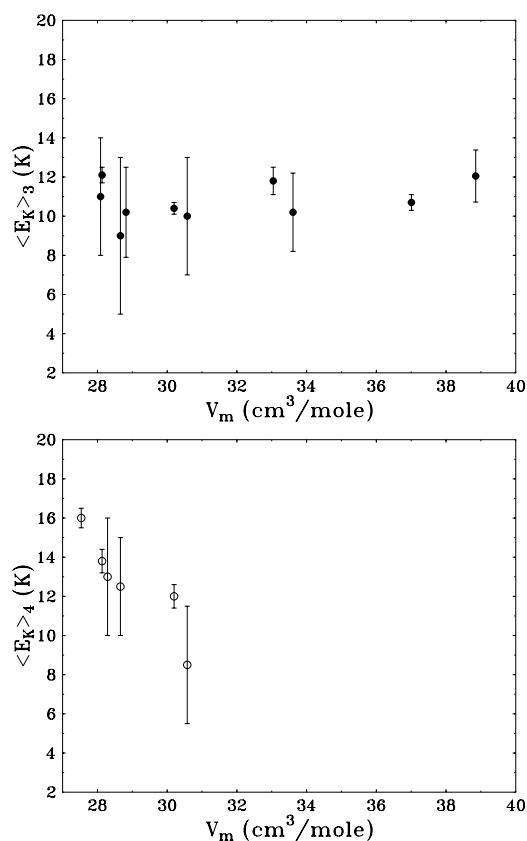


Figure 5. Mean kinetic energies $\langle E_K \rangle_3$ (top) and $\langle E_K \rangle_4$ (bottom) as a function of the molar volume in the mixtures. Values for $\langle E_K \rangle_3$ from the present work are at $V_m = 28.82$ and 38.852 $\text{cm}^3 \text{mol}^{-1}$, respectively. The remaining data are from [26, 27, 30].

mixtures and in the pure liquid. In the range $18 \text{ cm}^3 \text{mol}^{-1} \leq V_m \leq 40 \text{ cm}^3 \text{mol}^{-1}$, the pure liquid shows an increase in $\langle E_K \rangle_3$, while in the range $27 \text{ cm}^3 \text{mol}^{-1} \leq V_m \leq 40 \text{ cm}^3 \text{mol}^{-1}$, $\langle E_K \rangle_3$ is practically constant in the mixture. DINS results also show that $\langle E_K \rangle_3(x)$ is independent of molar volume and density n , which is quite a different behaviour from the widely assessed density dependence of the mean kinetic energy of all quantum fluids and solids. The kinetic energy of ^3He atoms appears unaffected by the presence of the higher-density boson fluid, which seems to promote ^3He delocalization. This picture suggests that the local environment of the ^3He atoms remains unchanged in saturated vapour pressure liquid mixtures. Although the measurements were carried out well above the stratification temperature of approximately 0.8 K [25], it appears that the local short-time behaviour of ^3He atoms is dominated by the existence of etherophases or ^3He clusters composed of a small number of atoms. This suggestion is, in some sense, similar to the results on low-density pure fluid ^3He , where the kinetic energy is lower than expected on the basis of mass difference arguments with respect to pure ^4He . Theoretical predictions on the mixtures, on the other hand, give values of $\langle E_K \rangle_3$ ranging from about 19 K for $x \rightarrow 0$ to about 12.7 K for $x = 1.00$ [18, 28]. As far as ^4He is concerned, values of $\langle E_K \rangle_4(x)$ in the mixture are similar to those in pure liquid for $x \rightarrow 0$ and they decrease as concentration increases (decreasing molar volume) (see figures 4 and 5), in agreement with theoretical predictions.

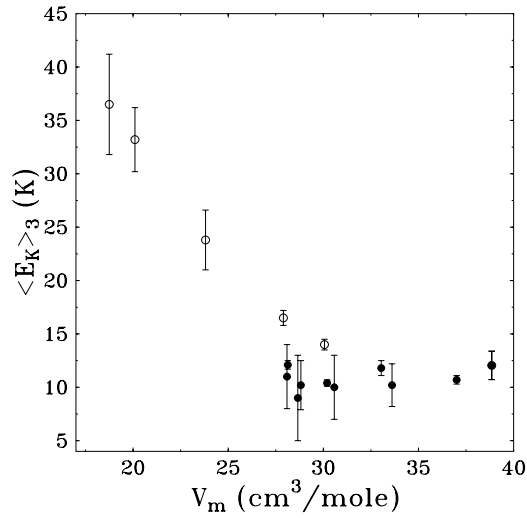


Figure 6. $\langle E_K \rangle_3$ as a function of the molar volume for pure ^3He (open circles) and for ^3He in the ^3He - ^4He mixture (solid circles).

Table 1. Deep inelastic neutron scattering determinations of He atomic kinetic energies, $\langle E_K \rangle_3$ and $\langle E_K \rangle_4$, as a function of ^3He concentration (x), temperature (T), and molar volume (V_m). Results from the present work (in bold) are at $T = 2.00$ K. The remaining data are from [26, 27, 30].

x	T (K)	V_m (cm ³ mol ⁻¹)	$\langle E_K \rangle_3$ (K)	$\langle E_K \rangle_4$ (K)
0.00	1.96	27.535	—	16.0 ± 0.5
0.096	1.4	28.29	11 ± 3	13.0 ± 3.0
0.10	1.96	28.133	12.1 ± 0.4	13.8 ± 0.6
0.15	1.4	28.659	9 ± 4	12.5 ± 2.5
0.20	2.00	28.82	10.2 ± 2.3	—
0.35	1.96	30.198	10.4 ± 0.3	12.0 ± 0.6
0.40	1.4	30.576	10 ± 3	8.5 ± 4.0
0.65	1.96	33.043	11.8 ± 0.7	—
0.70	1.4	33.610	10.2 ± 2.0	—
0.90	1.96	37.007	10.7 ± 0.4	—
1.00	2.00	38.852	12.05 ± 1.33	—

4. Conclusions

DINS is the most effective technique for determining momentum distributions and mean kinetic energies in condensed helium systems. A thorough insight into the short-time single-particle dynamics in these systems can be achieved through a systematic comparison of experimental results with sophisticated Monte Carlo simulations. Several aspects further stimulate experimental and theoretical studies, such as, for example, the momentum distribution in solid ^4He in the recently discovered supersolid phase [31], the condensate fraction in liquid ^3He - ^4He mixtures, the anharmonicities in solid ^3He - ^4He mixtures, and the nature of the molar volume dependence of kinetic energies. Yet liquid ^3He - ^4He mixtures represent a challenging benchmark system where the current picture of momentum distribution and kinetic energy in quantum fluids shows its limits. The results of the present work confirm that the effects of quantum statistics in the ^3He fermion component in the mixture show a departure from the

accepted density and molar volume dependence of the single-particle mean kinetic energy. Further measurements are underway in high-density liquid and solid ^3He - ^4He mixtures, aiming to accurately follow the changes of the momentum distribution and kinetic energy upon the reduction of particle exchange across the melting transition.

Acknowledgment

This work was supported within the CNR-CCLC agreement number 01/9001 concerning collaboration in scientific research at the spallation neutron source ISIS. The financial support of the Consiglio Nazionale delle Ricerche in this research is hereby acknowledged.

References

- [1] Dobbs E R 2000 *Helium Three* (Oxford: Oxford University Press)
- [2] Silver R N and Sokol P E 1989 *Momentum Distributions* (New York: Plenum)
- [3] Andreani C, Colognesi D, Mayers J, Reiter G F and Senesi R 2005 *Adv. Phys.* **54** 377
- [4] Watson G I 1996 *J. Phys.: Condens. Matter* **8** 5955–75
- [5] Glyde H R 1994 *Excitations in Liquid and Solid Helium* (Oxford: Clarendon)
- [6] Mayers J, Andreani C and Colognesi D 1997 *J. Phys.: Condens. Matter* **9** 10639–49
- [7] Senesi R, Andreani C, Colognesi D, Cunsolo A and Nardone M 2001 *Phys. Rev. Lett.* **86** 4584–7
- [8] Moroni S, Pederiva F, Fantoni S and Boninsegni M 2000 *Phys. Rev. Lett.* **84** 2650–3
- [9] Andreani C, Filabozzi A, Nardone M, Ricci F P and Mayers J 1994 *Phys. Rev. B* **50** 12744–6
- [10] Ceperley D M and Pollock E L 1986 *Phys. Rev. Lett.* **56** 351–4
- [11] Martel P, Svensson E C, Woods A D B, Sears V F and Cowley R A 1976 *J. Low Temp. Phys.* **23** 285–301
- [12] Ceperley D M, Simmons R O and Blasdell R C 1996 *Phys. Rev. Lett.* **77** 115–8
- [13] Ceperley D M 1995 *Rev. Mod. Phys.* **67** 279–355
- [14] Bafile U, Zoppi M, Barocchi F, Magli R and Mayers J 1995 *Phys. Rev. Lett.* **75** 1957–60
- [15] Sokol P E, Sköld K, Price D L and Kleb R 1985 *Phys. Rev. Lett.* **54** 909–12
- [16] Ceperley D M 1992 *Phys. Rev. Lett.* **69** 331–4
- [17] Azuah R T, Stirling W G, Guckelsberger K, Scherm R, Bennington S M, Yates M L and Taylor A D 1995 *J. Low Temp. Phys.* **101** 951–69
- [18] Mazzanti F, Polls A, Boronat J and Casulleras J 2004 *Phys. Rev. Lett.* **92** 085301
- [19] Colognesi D, Andreani C and Senesi R 2000 *Europhys. Lett.* **50** 202–8
- [20] Andreani C, Colognesi D, Degiorgi E, Filabozzi A, Nardone M, Pace E, Pietropaolo A and Senesi R 2003 Double difference method in deep inelastic neutron scattering on the VESUVIO spectrometer *Nucl. Instrum. Methods Phys. Res. A* **497** 535–49
- [21] Imberti S, Andreani C, Garbuio V, Gorini G, Pietropaolo A, Senesi R and Tardocchi M 2005 *Nucl. Instrum. Methods Phys. Res. A* **522** 463
- [22] Bafile U, Celli M, Zoppi M and Mayers J 1998 *Phys. Rev. B* **58** 791–7
- [23] Diallo S O, Pearce J V, Azuah R T and Glyde H R 2004 *Phys. Rev. Lett.* **93** 075301
- [24] Dimeo R, Sokol P E, Azuah R T, Bennington S M, Stirling W G and Guckelsberger K 1994 *Physica B* **241** 952
- [25] Kierstead H A 1976 *J. Low Temp. Phys.* **24** 497–512
- [26] Azuah R T, Stirling W G, Mayers J, Bailey I F and Sokol P E 1995 *Phys. Rev. B* **51** 6780–3
- [27] Wang Y and Sokol P E 1994 *Phys. Rev. Lett.* **72** 1040–3
- [28] Casulleras J and Boronat J 2000 *Phys. Rev. Lett.* **84** 3121–4
- [29] Glyde H R, Azuah R T and Stirling W G 2000 *Phys. Rev. B* **62** 14337–49
- [30] Senesi R, Andreani C, Fielding A L, Mayers J and Stirling W G 2003 *Phys. Rev. B* **68** 214522
- [31] Kim E and Chan M H W 2004 *Science* **305** 1941–4